

- [15] H. Kind, J. M. Bonard, L. Forro, K. Kern, K. Hernadi, L. O. Nilsson, L. Schluplach, *Langmuir* **2000**, *16*, 6877.  
 [16] S. Huang, A. W. H. Mau, T. W. Turney, P. A. While, L. Dai, *J. Phys. Chem. B* **2000**, *104*, 2193.  
 [17] A. M. Cassell, S. Verma, L. Delzeit, M. Meyyappan, J. Han, *Langmuir* **2001**, *17*, 260.  
 [18] S. Huang, L. Dai, A. W. H. Mau, *J. Phys. Chem. B* **1999**, *103*, 4223.  
 [19] C. Bower, W. Zhu, S. Jin, O. Zhou, *Appl. Phys. Lett.* **2000**, *77*, 830.  
 [20] X. B. Wang, Y. Q. Liu, D. B. Zhu, *Chem. Commun.* **2001**, *8*, 751.  
 [21] X. B. Wang, Y. Q. Liu, D. B. Zhu, *Adv. Mater.* **2002**, *14*, 165.  
 [22] X. B. Wang, Y. Q. Liu, D. B. Zhu, *Chem. Phys. Lett.* **2001**, *340*, 419.  
 [23] M. Yudasaka, R. Kikuchi, Y. Ohki, S. Yoshimura, *Carbon* **1997**, *35*, 195.  
 [24] H. Araki, H. Kajii, K. Yoshino, *Jpn. J. Appl. Phys. Pt. 2* **1999**, *38*, L836.  
 [25] C. J. Lee, D. W. Kim, T. J. Lee, Y. C. Choi, Y. S. Park, Y. H. Lee, W. B. Choi, N. S. Lee, G. S. Park, J. M. Kim, *Chem. Phys. Lett.* **1999**, *312*, 461.  
 [26] W. Yust, *Encyclopaedia Britannica*, Vol. 1, Encyclopaedia Britannica LTD, London **1955**.  
 [27] B. Q. Wei, R. Vajtai, Y. Jung, J. Ward, R. Zhang, G. Ramanath, P. M. Ajayan, *Nature* **2002**, *416*, 495.

## An Efficient Route to Graphitic Carbon-Layer-Coated Gallium Nitride Nanorods\*\*

By Weiqiang Han and Alex Zettl\*

The discovery of carbon nanotubes has inspired scientists to develop a range of potential applications.<sup>[1]</sup> Meanwhile, one- and two-dimensional GaN and its alloys with InN and AlN have attracted a great deal of attention, since the successful commercialization of bright blue light-emitting diodes, followed later by the demonstration of injection lasers.<sup>[2–4]</sup> GaN-based nitrides can be both p- and n-type doped, have direct bandgaps, and form heterostructures for device applications. There has recently been a great deal of interest in the preparation and characterization of nanotube-based nanocomposites to obtain unique physical and/or mechanical properties, since the properties become increasingly size dependent at low dimensions.<sup>[5–12]</sup> GaN-carbon composite nanotubes with carbon multilayers and GaN nanorods have been synthesized by an arc discharge method. The reaction is achieved by DC arc discharge between a graphite anode filled with a mixture of GaN, graphite, and nickel powders and a graphite cathode in a nitrogen atmosphere.<sup>[13]</sup> Although arc discharge is a widely used and simple way to generate a variety of carbon nanomaterials, there are disadvantages, such as low yield, poor purity, and poor reproducibility. In the production of GaN-carbon composite nanotubes, the number of carbon layers is usually large. Recently, Zhang et al. deposited thick graphitic layers on the surface of Si nanowires by using a hot filament chemical vapor deposition method.<sup>[14]</sup>

In this communication, we report the synthesis of GaN nanorods coated with graphitic carbon layers by the deposition of carbon layers (usually less than five), on pre-produced GaN nanorods using a conventional thermal chemical vapor deposition method.

GaN nanorods were prepared through a carbon nanotube-confined reaction.<sup>[4]</sup> Ga<sub>2</sub>O vapor was reacted with ammonia gas in the presence of carbon nanotubes at 950 °C to form GaN nanorods. The carbon nanotubes act as a template to confine the reaction. The nanorods have diameters of 5–60 nm and lengths of up to 30 μm. No residual carbon layers existed around the nanorods. The as-grown GaN nanorods were put in an alumina crucible, which was placed in the hot zone of a thermal chemical vapor deposition furnace, under flowing methane and at 900 °C for 15 min. The GaN nanorods, previously light yellow, turned black. The product was ultrasonically dispersed in ethanol and dropped on a holey carbon-coated grid for observation by high-resolution transmission electron microscopy (HRTEM) using a Philips CM200 FEG equipped with a parallel electron energy-loss spectroscopy detector (EELS, Gatan PEELS 678) and an energy-dispersive X-ray spectrometer (EDS).

HRTEM images of the sample show that most of the GaN nanorods have been covered with a few graphitic layers. Figure 1a is a low magnification TEM image of three nanorods covered with a few graphitic layers. Figure 1b is an enlarged image of the part of Figure 1a indicated by the arrow. It shows

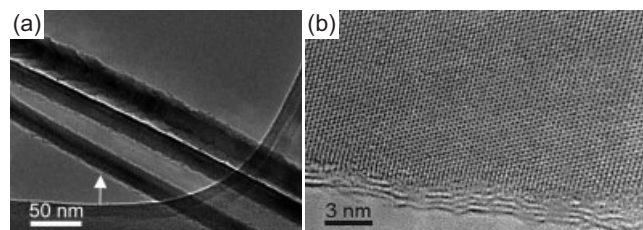


Fig. 1. a) Low-magnification TEM image of three nanorods covered with a few graphitic carbon layers. b) An enlarged image of (a) as indicated by the arrow.

that there are three layers covering the surface of the nanorod. The interlayer distances in the outer shells are about 0.36 nm, which is slightly larger than the value of the (002) spacing of hexagonal graphitic carbon and for carbon nanotubes. The carbon shells in this product had less than five layers for most of the coated nanorods examined. The carbon layers extended all along the nanorod and adhered well to the surface. Their structure could be perfect or distorted. EDS shows that Ga, N, and C are present in the composite nanotubes (Fig. 2a). A typical EELS spectrum from an individual composite nanotube is shown in Figure 2b (curve 1). K-edge absorption for carbon and nitrogen, whose distinct absorption features start at 284 eV and 401 eV, respectively, are revealed in the spectrum. To determine whether carbon is in the core or not, we removed the carbon layers by condensing the electron beam of the microscope onto the carbon layers. After irradiation for several minutes, we found that the carbon layers had mostly been removed, but the nanorod was still left. We

[\*] Prof. A. Zettl, Dr. W. Han  
 Department of Physics, University of California  
 Berkeley, CA 94720 (USA)  
 and  
 Materials Science Division, Lawrence Berkeley National Laboratory  
 Berkeley, CA 94720 (USA)  
 E-mail: azettl@physics.berkeley.edu

[\*\*] We thank C. Nelson for help with TEM measurements. This research was supported in part by the Office of Energy Research, Office of Basic Energy Science, Division of Materials Sciences, U.S. Department of Energy (contract DE-AC03-76SF00098), and NSF grants DMR-9801738.

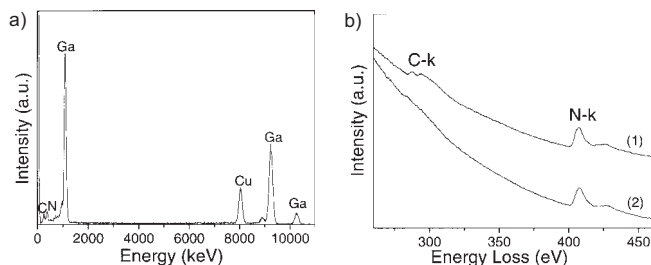


Fig. 2. a) Typical EDS spectrum of a carbon-coated nanorod. b) Curve 1 is an EELS spectrum of the core electron K-shell for carbon and nitrogen; curve 2 is the corresponding EELS spectrum from the same area after the covered carbon layers have been removed by electron irradiation.

took the EELS spectrum (curve 2 in Fig. 2b) once again in the same area and found that the C peak had almost disappeared. From this result, we know that carbon is in the outer layers and the core is GaN, although there is still a possibility that a very small amount of carbon is in the GaN core. Figure 3a shows a high-resolution image of a carbon-coated nanorod with a single carbon layer covering the surface of a GaN nanorod of diameter  $\sim 13$  nm. The composite nanotube

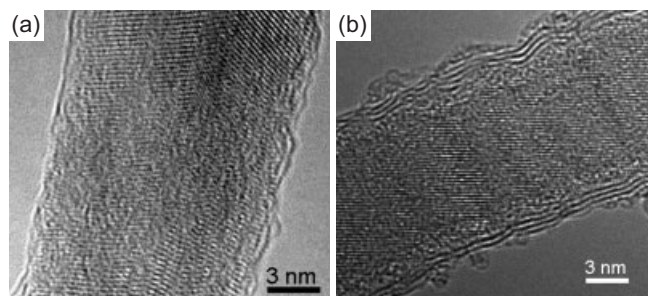


Fig. 3. a) High-resolution image of a carbon-coated nanorod with one single carbon layer covering the surface of a GaN nanorod. b) Carbon-coated nanorod with three carbon layers covering the surface of GaN nanorod.

was tilted by  $55^\circ$  about the tube axis, and it was found that the single layer fully covered the surface. Figure 3b shows a high-resolution image of a coated nanorod with three carbon layers covering the surface of a GaN nanorod of diameter  $\sim 10$  nm. Some very small fullerene-like nanoparticles are also pasted on the surface of the carbon layers. Figure 4a shows a low-magnification image of a coated nanorod with saw-like edges on both the carbon layers and the GaN nanorod. Figure 4b is an enlarged image of the part of Figure 4a indicated by the arrow. This shows that the morphology of the carbon layers can be straight or curved and is dependent on the morphology of the GaN nanorods.

As a comparison, control experiments under the same experimental conditions reported above were performed with ethane instead of methane and with deposition temperatures ranging from  $700\text{--}1000^\circ\text{C}$ . Only small amounts of GaN nanorods were covered with carbon layers. Methane is known to be the most kinetically stable hydrocarbon and undergoes the least pyrolytic decomposition at high temperature; therefore it can be used to grow single-walled and double-walled nanotubes using metal oxide as catalyst.<sup>[15]</sup> Our experiments show

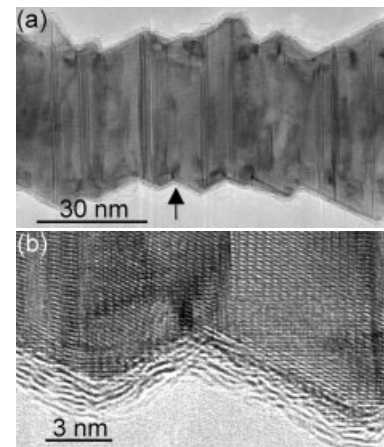


Fig. 4. a) Carbon-coated GaN nanorod with saw-like edges. b) Enlarged image of (a) as indicated by the arrow.

that the number of carbon layers can be controlled, to less than five layers, by using methane as the hydrocarbon source.

By hot filament chemical vapor deposition of carbon on the surface of a Si nanorod, Zhang et al. reported that when the temperature was as high as  $1000^\circ\text{C}$ , the Si cores tended to transform into SiC cores and the carbon layers grown on the SiC cores were distorted.<sup>[14]</sup> It is well known that GaN does not react with carbon, although very small amounts of carbon might be incorporated into GaN as dopant.<sup>[3]</sup> Our experiment has shown that both the composition and the morphology of GaN do not change during carbon layer deposition.

Fabrication of nanocomposites based on the tailored morphology of nanorods provides a unique template-based process for making nanocomposite materials with carbon layers. Graphitic carbon layers can act as chemically inert protecting layers for gallium nitride nanorods. We note that the TEM studies show explicitly that carbon-coated GaN nanorods are far less susceptible to electron-beam damage than uncoated GaN nanorods. Specifically, under beam-condensed 200 kV electron irradiation, the lifetime of a typical 30 nm diameter nanorod is approximately doubled with the addition of four carbon layers. The lifetime is increased further with the addition of more carbon layers. We also expect other beneficial effects of carbon coating, such as enhanced stability, for example, of such nanorods against photobleaching, when used as solid-state injection nanolasers. The physical properties of the graphitic carbon-coated gallium nanorods can be speculated to be, in general, very interesting.

Received: January 15, 2002  
Final version: August 5, 2002

- [1] S. Iijima, *Nature* **1991**, 354, 56.
- [2] S. Nakamura, T. Mukai, M. Senoh, *Appl. Phys. Lett.* **1994**, 64, 1687.
- [3] G. Popovici, H. Morkoc, S. N. Mohammad, in *Group III Nitride Semiconductor Compounds* (Ed: B. Gil), Clarendon Press, Oxford **1998**, Ch. 2.
- [4] W. Han, S. Fan, Q. Li, Y. Hu, *Science* **1997**, 277, 1287.
- [5] P. M. Ajayan, P. Redlich, M. Rühle, *J. Microsc.* **1997**, 185, 275.
- [6] J. Sloan, J. Cook, M. L. H. Green, J. L. Hutchison, R. Tenne, *J. Mater. Chem.* **1997**, 7, 1089.
- [7] Y. Zhang, K. Suenaga, C. Colliex, S. Iijima, *Science* **1998**, 68, 293.
- [8] W. Han, P. Redlich, F. Ernst, M. Rühle, *Chem. Mater.* **1999**, 11, 3620.
- [9] W. Han, P. Redlich, F. Ernst, M. Rühle, *Appl. Phys. Lett.* **1999**, 75, 1875.

- [10] M. Terrones, W. K. HsuHsu, H. W. Kroto, D. R. M. Walton, *Top. Curr. Chem.* **1999**, *199*, 189.  
 [11] W. Q. Han, P. Kohler-Redlich, C. Scheu, F. Ernst, M. Rühle, N. Grobert, M. Terrones, H. W. Kroto, D. R. W. Walton, *Adv. Mater.* **2000**, *12*, 1356.  
 [12] W. S. Shi, H. Y. Peng, L. Xu, N. Wang, Y. H. Tang, S. T. Lee, *Adv. Mater.* **2000**, *12*, 1927.  
 [13] W. Han, P. Redlich, F. Ernst, M. Rühle, *Appl. Phys. Lett.* **2000**, *76*, 652.  
 [14] Y. F. Zhang, Y. H. Tang, Y. Zhang, C. S. Lee, I. Bello, S. T. Lee, *Appl. Phys. Lett.* **2000**, *330*, 48.  
 [15] J. Kong, A. M. Cassell, H. Dai, *Chem. Phys. Lett.* **1998**, *292*, 567.

## Protein Cage Constrained Synthesis of Ferrimagnetic Iron Oxide Nanoparticles\*\*

By Mark Allen, Debbie Willits, Jesse Mosolf, Mark Young,\* and Trevor Douglas\*

The field of biomineralization has highlighted the possibilities of materials synthesis based on molecular interactions between supramolecular organic assemblies and inorganic materials.<sup>[1]</sup> For example, the protein assembly of the iron storage protein, ferritin, provides a size-constrained reaction for the synthesis of both natural and synthetic inorganic nanomaterials.<sup>[2–7]</sup> Similarly, it has been shown that the protein cage structures of viruses can act as a constrained reaction environment for nanomaterials synthesis,<sup>[8,9]</sup> and that the protein can be modified to alter the mineralization specificity.<sup>[10]</sup> In both the virus and the synthetic ferritin systems, the interior surfaces have regions of high charge density, which act as sites for synthetic mineral nucleation. The utility of this approach to nanomaterials synthesis lies in the molecular nature of these cage-like architectures, which results in the formation of size-constrained materials with narrow size distributions. Here we report on the use of a twelve subunit protein cage for the constrained synthesis of ferrimagnetic iron oxide nanoparticles of 5 nm diameter.

The unusual ferritin-like protein from the bacteria *Listeria innocua* has been shown to form a twelve subunit cage structure surrounding a 5 nm diameter interior cavity.<sup>[11,12]</sup> This small cage structure has the capacity to hold only 500 Fe atoms as a nanoparticle of a ferric oxyhydroxide.<sup>[13,14]</sup> This cage provides a new size regime for nanomaterials synthesis that approaches the molecular size regime and holds the promise for fine tuning size-dependent materials properties. In the present work we have cloned the ferritin-like protein (FLP) from *L. innocua* into an *E. coli* expression system, and used the overexpressed recombinant protein cage for the size-

constrained synthesis of nanoparticles of the ferrimagnetic iron oxide maghemite ( $\gamma\text{-Fe}_2\text{O}_3$ ).

The FLP from the bacteria *Listeria innocua* was cloned into an inducible *E. coli* heterologous expression system. The FLP was purified as previously described and analyzed by size exclusion chromatography (SEC), transmission electron microscopy (TEM), and dynamic light scattering (DLS). SEC indicated an assembled protein with a  $M_w$  of 220 kDa. Protein samples negatively stained with uranyl acetate and imaged by TEM revealed a cage-like structure, with an outer diameter of  $8.5 \pm 0.6$  nm, and an inner diameter of approximately 5 nm (Fig. 1a). The dimensions of the recombinant protein cages were confirmed by DLS, which indicated a particle diameter of  $9.2 \pm 0.4$  nm (Fig. 1b).

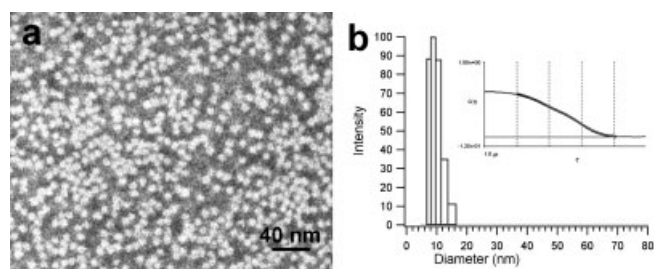
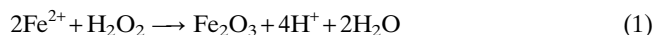


Fig. 1. a) TEM of the *L. innocua* FLP cage purified from *E. coli*, stained with uranyl acetate, and b) DLS of the purified recombinant *L. innocua* FLP cage (inset: correlation function and fit).

The *L. innocua* FLP has previously been shown to mineralize Fe as a nanoparticle of an as-yet-unidentified ferric oxyhydroxide.<sup>[13,14]</sup> Thus it is clear that under physiological conditions the protein can process  $\text{Fe}^{\text{II}}$  to form size-constrained materials. We have investigated the Fe mineralization in the FLP cage under the non-physiological conditions of elevated temperature and pH and controlled oxidation. We have shown that the FLP will mineralize nanoparticles of  $\gamma\text{-Fe}_2\text{O}_3$  encapsulated within the protein cage. Treatment of the protein at pH 8.5 and  $65^\circ\text{C}$  with 400  $\text{Fe}^{\text{II}}$  per protein and substoichiometric amounts of  $\text{H}_2\text{O}_2$  resulted in the formation of a homogeneous solution with a deep-brown coloration. The reaction was run unbuffered and the  $\text{H}^+$  generated as a result of the oxidative hydrolysis reaction was monitored and titrated dynamically to maintain the reaction at pH 8.5. In this way we could quantify the reaction stoichiometry and determine that two equivalents of  $\text{H}^+$  were liberated per  $\text{Fe}^{\text{II}}$ , consistent with Reaction 1.



When negatively stained with uranyl acetate and imaged by TEM, mineralized preparations of the *L. innocua* FLP demonstrated that the intact protein cages surrounded the mineral nanoparticle (Fig. 2a). The iron oxide nanoparticles could be imaged in unstained mineralized samples as shown in Figure 2b. The measured iron oxide mineral particle size ( $4.1 \pm 1.1$  nm diameter) is consistent with the interior dimensions of the protein cage. Selected area diffraction collected

[\*] Prof. T. Douglas, M. Allen, J. Mosolf  
 Department of Chemistry and Biochemistry, Montana State University  
 Bozeman, MT 59717 (USA)  
 E-mail: tdouglas@chemistry.montana.edu

Prof. M. Young, D. Willits  
 Department of Plant Sciences, Montana State University  
 Bozeman, MT 59717 (USA)  
 E-mail: myoung@montana.edu

[\*\*] This work was funded by a grant from the NSF. We thank Sue Brumfield for assistance with electron microscopy.